PHYSICAL REVIEW C **73**, 051603(R) (2006)

Radial sensitivity of elastic scattering at near barrier energies for weakly bound and tightly bound nuclei

D. Roubos,[1] A. Pakou,[1,*] N. Alamanos,[2] and K. Rusek[3]
[1]*Department of Physics, The University of Ioannina, GR-45110 Ioannina, Greece*
[2]*CEA-Saclay, DAPNIA-SPhN, Gif-sur-Yvette, France*
[3]*Department of Nuclear Reactions, Andrzej Sołtan Institute for Nuclear Studies, Hoża 69, PL-00681 Warsaw, Poland*
(Received 25 January 2006; published 31 May 2006)

The radial sensitivity of elastic scattering for weakly bound (^{6}Li, ^{7}Li, ^{9}Be) and tightly bound projectiles (^{12}C, ^{16}O) on light and heavy targets (^{28}Si, ^{58}Ni, ^{118}Sn, ^{208}Pb, ^{209}Bi) is sought at barrier energies, taking into account a Woods -Saxon potential and a BDM3Y1 interaction. The results are discussed in terms of the potential anomaly at the coulomb barrier.

DOI: 10.1103/PhysRevC.73.051603 PACS number(s): 27.20.+n, 25.70.Bc, 24.10.Ht

Coupled channel effects have been a popular subject for several decades. Today, the subject is again of particular interest for the case of weakly bound nuclei involved in reactions at the barrier. The potential threshold anomaly is an effect with consequences on the reaction channel mechanisms in this energy region. The term "threshold anomaly" [1,2] was invoked to describe, for tightly bound nuclei, the rapid energy variation of the real and imaginary part of the potential in the region around the Coulomb barrier; this variation is visualized as a peak in the real part associated with a sharp decrease with falling energy in the strength of the imaginary potential. For weakly bound systems, however, the situation, which has been recently outlined in [3,4], is more complicated.

The quantities obtained in the above studies are the real and imaginary potentials as a function of energy in the vicinity of the barrier. It is customary to obtain such quantities at the strong absorption radius. As discussed in [4], however, the radial region of sensitivity may change with bombarding energy for lighter systems. Additionally, as pointed out in [5–7], the reduced interaction distance of the closest approach for the systems ^{6}He+^{208}Pb and ^{6,7}Li+^{28}Si is ∼2.2 fm instead of ∼1.65 fm, a value which has been obtained for several stable systems [7,8]. It is therefore important to know what radial region of the nuclear potential can be considered to be well mapped by the analysis of elastic scattering data.

In this context, we have studied several weakly bound and tightly bound projectiles, elastically scattered by light and heavy targets, in order to determine the radial region of the potential sensitivity.

We adopt the technique outlined, e.g., in [9] taking into account a Woods-Saxon potential. The radius of sensitivity is searched by fitting V_0 and W_0 at different diffusivities in the region $\alpha_{V(W)} = 0.40$ to 0.80 and by fixing the reduced radii $r_{0V(W)}$ at previously found best values. The elastic scattering of the following systems is considered at near barrier energies: (^{6}Li, ^{7}Li, ^{9}Be) and (^{12}C, ^{16}O) on light and heavy targets (^{28}Si,^{58}Ni, ^{118}Sn, ^{208}Pb, ^{209}Bi). Data are taken from [3,4,10–21]. As an example, some results for the real part of the potential of the systems ^{6}Li+^{208}Pb and ^{16}O+^{208}Pb are presented in Figs. 1 and 2 for various energies. The best fit parameters for the barrier energy are given in Tables I and II. The phenomenon outlined in these figures is that at near barrier energies [Figs. 1(b)–(1)d and 2(b)–2(d)], the tightly bound projectiles, in principle, probe a unique radius of the potential, which is almost equal to the strong absorption radius (details can be found in Ref. [23]), that is, the radius at the point where the ratio of elastic scattering to Rutherford scattering drops to 0.25. For the weakly bound projectiles, the behavior is slightly different. The probed radii are located in the vicinity of the strong absorption radius, but these values are larger by ∼9% than the strong absorption radius for heavy targets and by ∼19% for the light ones. Radii of the potential sensitivity for ^{6}Li+^{208}Pb and ^{16}O+^{208}Pb are compared in Fig. 3, with two extreme radii: the strong absorption radius and the interaction distance at the point where the above ratio drops slightly from unity to 0.98. The latter ratio is chosen so as to comply with previous definitions in publications [5–7]. The analysis for the interaction distances is done according to [5]. A table, with the sensitive radii and strong absorption radii and radii at the ratio 0.98, for all the systems considered in this work, is given in Ref. [23]. It should be noted that for the imaginary potential, crossings occur at smaller separations and occasionally are not well defined. The same result is also reported by other authors [21].

On the other hand at the barrier [Figs. 1(a) and 2(a)], two crossings are observed at two distinct radii. The first is associated with high absorption and corresponds to a small radius, while the second is associated with low absorption and corresponds to a large radius. We claim that the first crossing is due to farside scattering; the second, to nearside scattering. We also claim that the appearance of two crossings is due to a possible "decoupling" of the nearside scattering, dominated by the Coulomb repulsion, and the farside scattering, due to the strong attractive nuclear potential. By "decoupling" we mean that at these low energies, the farside scattering is so weak that no observable interference effects occur with the nearside scattering.

In order to support the above argument, we proceed with the following analysis. In a first step, we take as example the ^{6}Li+^{208}Pb elastic scattering at barrier energy

*Corresponding author: apakou@cc.uoi.gr

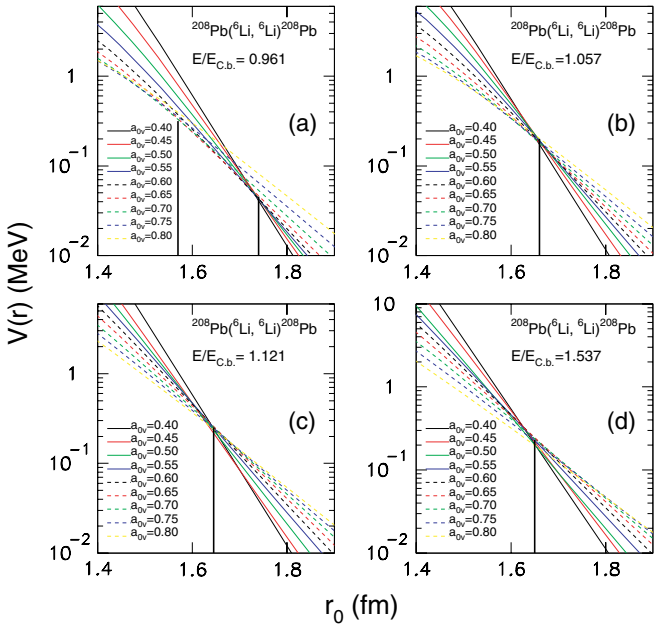

FIG. 1. (Color online) Radial sensitivity for the system ^{6}Li+^{208}Pb at various energies near the Coulomb barrier with the crossing technique. Real potential $V(r)$ is plotted as a function of the reduced radius r_0. Coulomb barrier energy $E_{\mathrm{C.b.}}$ is calculated according to Broglia and Winther [22] and is 30.35 MeV.

$(E/E_{\mathrm{C.b.}} = 0.96)$ and we decompose the angular distribution for the best fitted Woods-Saxon potential [Fig. 1(a)] in two parts. One originating from nearside scattering and one from farside scattering. The results are presented in Fig. 4(a). As expected, the farside scattering is almost negligible for the more forward angles, more specifically for angles up to the point where the ratio of the angular distribution to Rutherford

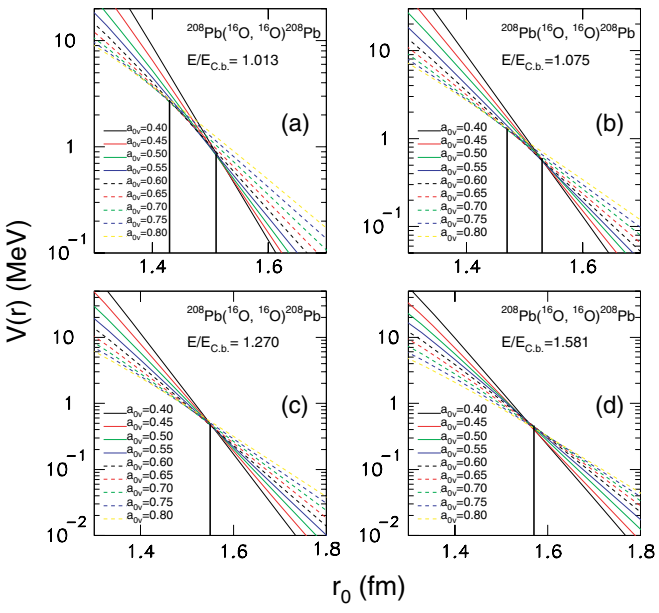

FIG. 2. (Color online) Same as Fig. 1, but for ^{16}O+^{208}Pb and $E_{\mathrm{C.b.}}$ 76.05 MeV.

TABLE I. Best fit parameters for the ^{6}Li+^{208}Pb potentials at $E/E_{\mathrm{C.b.}} = 0.96$, appearing in Fig. 1(a) with $r_V = r_W = 1.34$ fm.

V_0 (MeV)	W_0 (MeV)	$\alpha_V = \alpha_W$(fm)	χ^2/ν
114.03	123.24	0.40	2.21
49.93	75.55	0.45	2.02
24.66	48.37	0.50	1.83
13.67	32.46	0.55	1.67
8.59	22.72	0.60	1.53
6.16	16.47	0.65	1.42
5.02	12.29	0.70	1.34
4.54	9.38	0.75	1.29
4.41	7.29	0.80	1.26

drops to $\sim$0.60. On the other hand, near the barrier at $E/E_{\mathrm{C.b.}} = 1.12$, the farside contribution starts to grow, and interference effects can be stronger [Fig. 4(b)]. As a second step, we perform an analysis of the barrier energy angular distribution, selecting data at the forward angles, starting with the more forward ones, and subsequently increasing the angular range. It is found that up to the angle where the ratio of elastic to Rutherford scattering drops to 0.60, only one crossing occurs, which is associated with the large radius and small absorption. Therefore, according to our calculations presented in Fig. 4(a), this corresponds mainly to nearside scattering. This analysis is repeated for all the systems considered within this work. The two-crossing effect at the barrier is obvious for all the projectiles, weakly and tightly bound, on heavy targets. The results on light targets are, however, less convincing. Unfortunately, the lists of data that we possess do not contain systematic data at very backward angles, or the quality of the fits is not always good enough to isolate also the crossing of farside scattering. We have, however, attempted to do it with the system ^{6}Li+^{208}Pb, where the quality of the data is excellent and the number of data points is large. The results are presented in Fig. 5. Note that the analysis including data only at the forward angles probes only one crossing, which corresponds to low diffusivity and the large radius. The analysis including data only at the backward angles also probes only one crossing, but which now corresponds to high diffusivity and the short radius.

TABLE II. Best fit parameters for the ^{16}O+^{208}Pb potentials at $E/E_{\mathrm{C.b.}} = 1.013$, appearing in Fig. 2(a), with $r_V = r_W = 1.20$ fm.

V_0 (MeV)	W_0 (MeV)	$\alpha_V = \alpha_W$(fm)	χ^2/ν
757.55	532.83	0.40	1.38
342.17	254.33	0.45	1.93
186.68	136.54	0.50	2.62
117.40	80.31	0.55	3.43
82.12	50.94	0.60	4.34
62.33	34.19	0.65	5.32
50.39	24.01	0.70	6.35
42.80	17.48	0.75	7.40
37.76	13.11	0.80	8.45

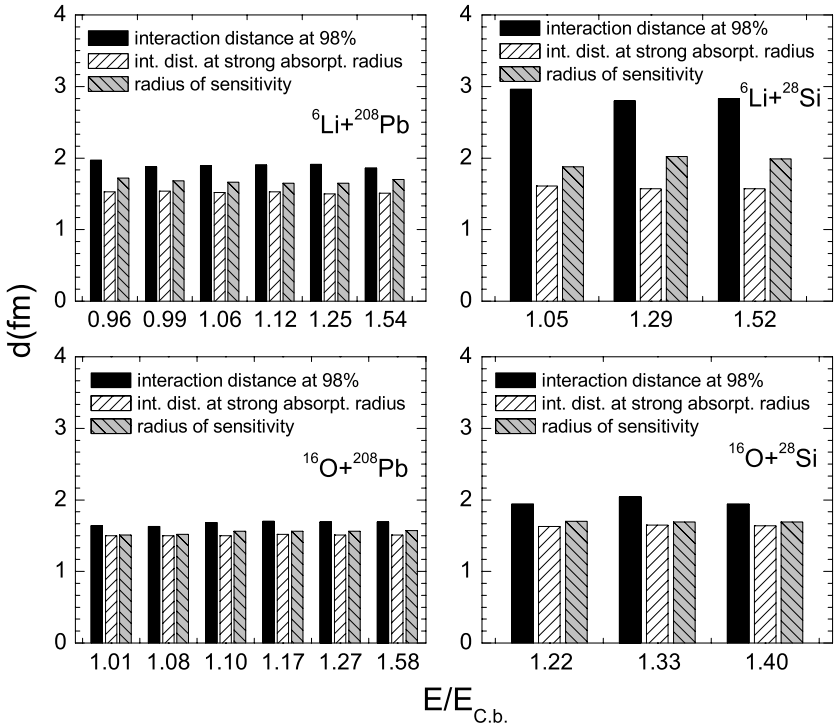

FIG. 3. Reduced sensitive radii (grey bars with diagonal lines) for the ^{6}Li+^{208}Pb, ^{6}Li+^{28}Si (top figures) and ^{16}O+^{208}Pb, ^{16}O+^{28}Si (bottom figures) potentials as a function of reduced energy are compared with reduced interaction distances at the point where the ratio of elastic scattering to Rutherford scattering drops to 25% (strong absorption radius, white bars with diagonal lines) and at the point where the above ratio drops to 98% (black bars). Note that the sensitive radius at the barrier was taken as the mean of the two separations corresponding to the two observed crossings.

Another interesting point which should be noted is that for the weakly bound projectile ^{6}Li, the small separation corresponds to the strong absorption radius and is associated with high absorption (farside scattering), while the larger separation (nearside scattering) corresponds to an interaction distance at a point where the elastic scattering drops slightly from the Rutherford scattering and is associated with low absorption. In contrast, for tightly bound nuclei and the less

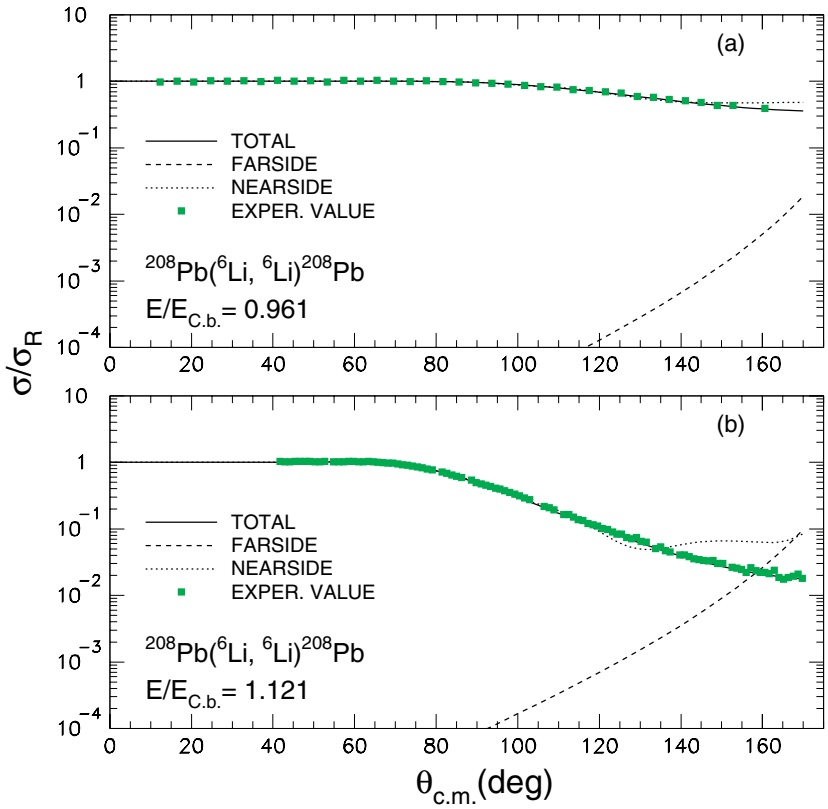

FIG. 4. (Color online) Elastic scattering angular distributions for ^{6}Li+^{208}Pb (a) at barrier and (b) near barrier energies. Curves are optical model calculations with a Woods-Saxon potential (best fit solid line). Decomposition of the farside (dashed line) and nearside (dotted line) scattering is also shown.

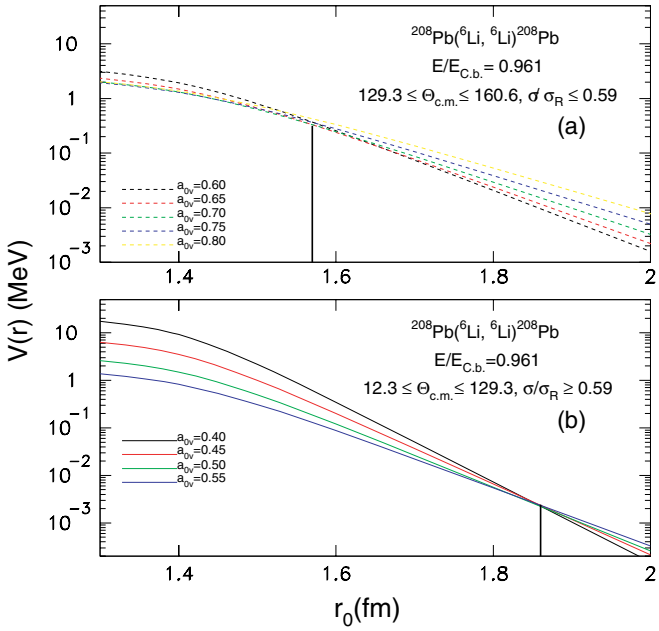

FIG. 5. (Color online) Presentation of the two-crossing effect due to a possible decoupling of farside and nearside sacttering. Data at backward angles (a) probe the short radius connected with high diffusivity; data at forward angles (b) probe the large radius connected with low diffusivity. Potential lines with low diffusivity (a) and high diffusivity (b) do not converge in a crossing and were omitted.

weakly bound ^{7}Li and ^{9}Be, the small separation goes even deeper than the strong absorption radius, while the large separation lies beyond but closer to the strong absorption radius.

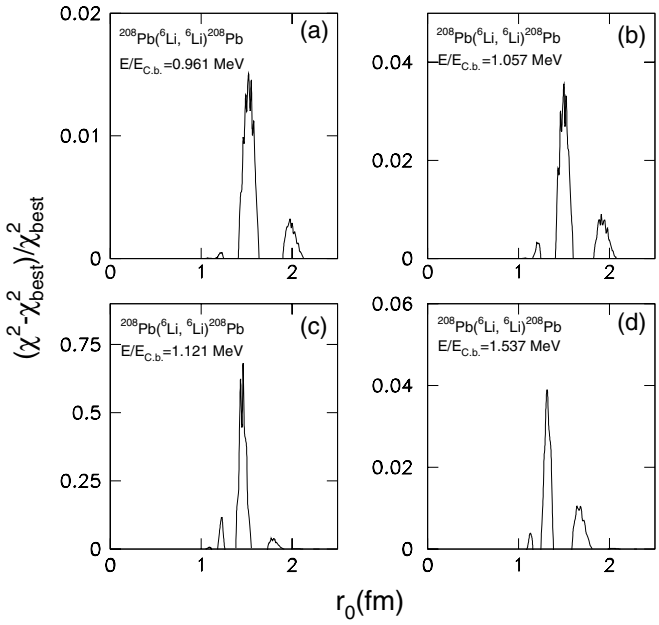

FIG. 6. Same as Fig. 1, but with the notch technique. Relative χ^2 change is plotted vs reduced radius.

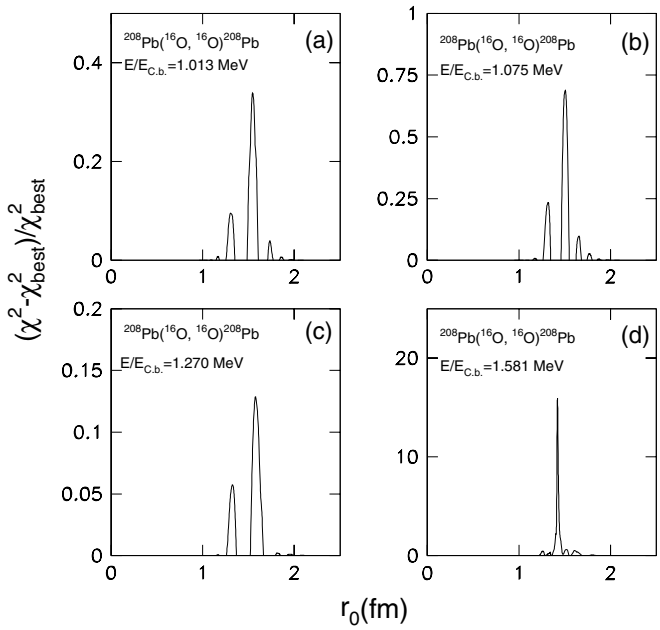

FIG. 7. Same as Fig. 2, but with the notch technique. Relative χ^2 change is plotted vs reduced radius.

Similar results are obtained by using the density-dependent BDM3Y1 interaction [24] and the notch technique [25,26]. A dip with a width of 0.2 fm is formed in the potential at a radius $r = R$ by multiplying the potential by 0.8. Then the dip is moved across the potential, and the relative change of χ^2 is plotted as a function of the reduced radius r_0. The results plotted in Figs. 6 and 7 show that for the weakly bound nuclei, the sensitive region extends well into the surface up to a reduced radius of 2 fm, with the most sensitive region close to the strong absorption radius. For the stable nuclei, the sensitive region moves even deeper than the strong absorption radius, while it extends weakly to the surface up to 1.7 fm. Note that for light targets the situation is the same for both tightly bound and weakly bound projectiles and follows the behavior of the weakly bound nuclei on heavy targets.

In conclusion, then, with respect to the potential anomaly at the Coulomb barrier, to make meaningful comparisons between tightly bound and weakly bound nuclei, it is necessary to plot the potential at the appropriate radius. In this work we found that for the tightly bound nuclei, the appropriate radius is the strong absorption radius, whereas the same does not hold for the weakly bound ones. In the latter case, the sensitive radius is ∼9% higher than the strong absorption radius for scattering on heavy targets and ∼19% higher for scattering on light targets. Therefore, it is necessary to perform a radial sensitivity analysis in advance of plotting the potential.

We also addressed a two-crossing effect at the barrier, which may be attributed to a possible decoupling of farside and nearside scattering. More calculations and/or experiments are necessary, however, in order to fully explore and prove this argument.

[1] G. R. Satchler, Phys. Rep. **199**, 147 (1991).
[2] C. Mahaux, H. Ngo, and G. R. Satchler, Nucl. Phys. **A449**, 354 (1986).
[3] A. Pakou *et al*., Phys. Lett. **B556**, 21 (2003).
[4] A. Pakou *et al*., Phys. Rev. C **69**, 054602 (2004).
[5] Athena Pakou and Krzysztof Rusek, Phys. Rev. C **69**, 057602 (2004).
[6] B. T. Kim, W. Y. So, S. W. Hong, and T. Udagawa, Phys. Rev. C **65**, 044616 (2002).
[7] B. T. Kim, W. Y. So, S. W. Hong, and T. Udagawa, Phys. Rev. C **65**, 044607 (2002).
[8] P. R. Christensen, V. I. Manko, F. D. Becchetti, and R. J. Nickles, Nucl. Phys. **A207**, 33 (1973).
[9] A. Zerwekh *et al*., Phys. Rev. C **58**, 3445 (1998).
[10] K. O. Pfeiffer, E. Speth, and K. Bethge, Nucl. Phys. **A206**, 545 (1973).
[11] A. M. M. Maciel *et al*., Phys. Rev. C **59**, 2103 (1999).
[12] C. Signorini *et al*., Phys. Rev. C **67**, 044607 (2003).
[13] N. Keeley *et al*., Nucl. Phys. **A571**, 326 (1994).
[14] J. S. Eck, T. J. Gray, and R. K. Gardner, Phys. Rev. C **16**, 1873 (1977).
[15] S. B. Moraes *et al*., Phys. Rev. C **61**, 064608 (2000).
[16] R. J. Woolliscroft *et al*., Phys. Rev. C **69**, 044612 (2004).
[17] C. Signorini *et al*., Phys. Rev. C **61**, 061603(R) (2000).
[18] F. Videbaek *et al*., Phys. Rev. C **15**, 954 (1977).
[19] St. C. Pieper *et al*., Phys. Rev. C **18**, 180 (1978).
[20] J. B. Ball *et al*., Nucl. Phys. **A252**, 208 (1975).
[21] C. Tenreiro *et al*., Phys. Rev. C **53**, 2870 (1996).
[22] Ricardo A. Broglia and Aage Winther, *Heavy Ion Reactions, Vol. I, Elastic and Inelastic Reactions* (Benjamin-Cummings, Redwood City, CA, 1981).
[23] See EPAPS Document No. E-PRVCAN-73-015606 for tables with sensitive radii strong absorption radii at the point where the elastic scattering over Rutherford drops to 0.98. For more information on EPAPS, see http://www.aip.org/pubservs/epaps.html.
[24] D. T. Khoa and W. von Oertzen, Phys. Lett. **B342**, 6 (1995).
[25] J. G. Cramer and R. M. De Vries, Phys. Rev. C **22**, 91 (1980).
[26] K. Rusek *et al*., Nucl. Phys. **A407**, 208 (1983).